What drives the electrodynamics of the low-latitude evening ionosphere?

Arthur D. Richmond[1], William Evonosky[2], Tzu-Wei Fang[3], Astrid Maute[1]

[1]High Altitude Observatory, National Center for Atmospheric Research
[2]Department of Physics, University of South Florida
[3]Cooperative Institute for Research in Environmental Sciences, University of Colorado

Neutral and plasma dynamics are strongly coupled in the F region. In the low-latitude evening ionosphere an eastward neutral wind is accelerated by a strong eastward horizontal pressure gradient force that is incompletely balanced by ion drag and viscosity. Plasma convection is driven mainly by the zonal neutral wind in the lower Equatorial Ionization Anomaly (EIA) region, balanced by ion-neutral collisions in the E and lower F regions. Increased night-time E-region conductivity retards both ion convection and neutral winds in the F region. Unless the E-region night-time conductivity is large, the accelerating eastward ion convection draws plasma up from lower apex heights, producing the equatorial F-region pre-reversal enhancement of vertical ion drift.

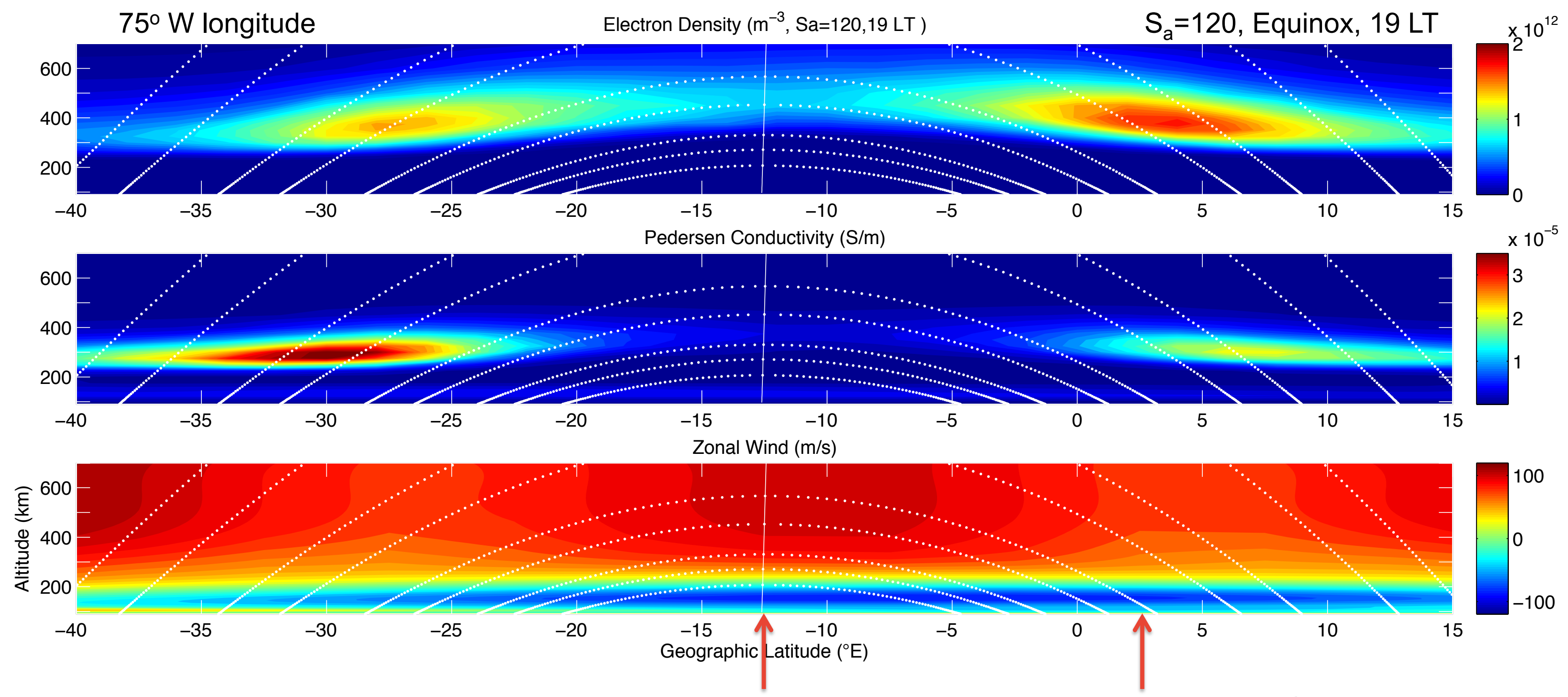

1. Low-latitude electron density, Pedersen conductivity, and eastward wind simulated with the coupled Global Ionosphere-Plasmasphere (GIP) model and Thermosphere-Ionosphere-Electrodynamics General Circulation Model (TIEGCM) for equinox, medium solar activity, 0 UT, 75°W longitude (19 LT), with equal scales for latitudinal distance and height. Dotted lines are geomagnetic field lines. The nearly vertical lines around −12.5° latitude trace the magnetic equator with altitude.

- Electron density shows Equatorial Ionization Anomaly (EIA) maxima around 15° either side of magnetic equator.
- Pedersen conductivity maximizes in lower/poleward region of the EIA in electron density, and has weak E-region layer.
- Wind is eastward above 200 km, and westward below.
- Eastward wind is reduced in EIA regions. Momentum is transferred to lower altitudes, where wind is weaker or negative.
- Vertical arrows are latitudes for which vertical profiles of wind and neutral-ion collision frequency are shown in Fig. 4.

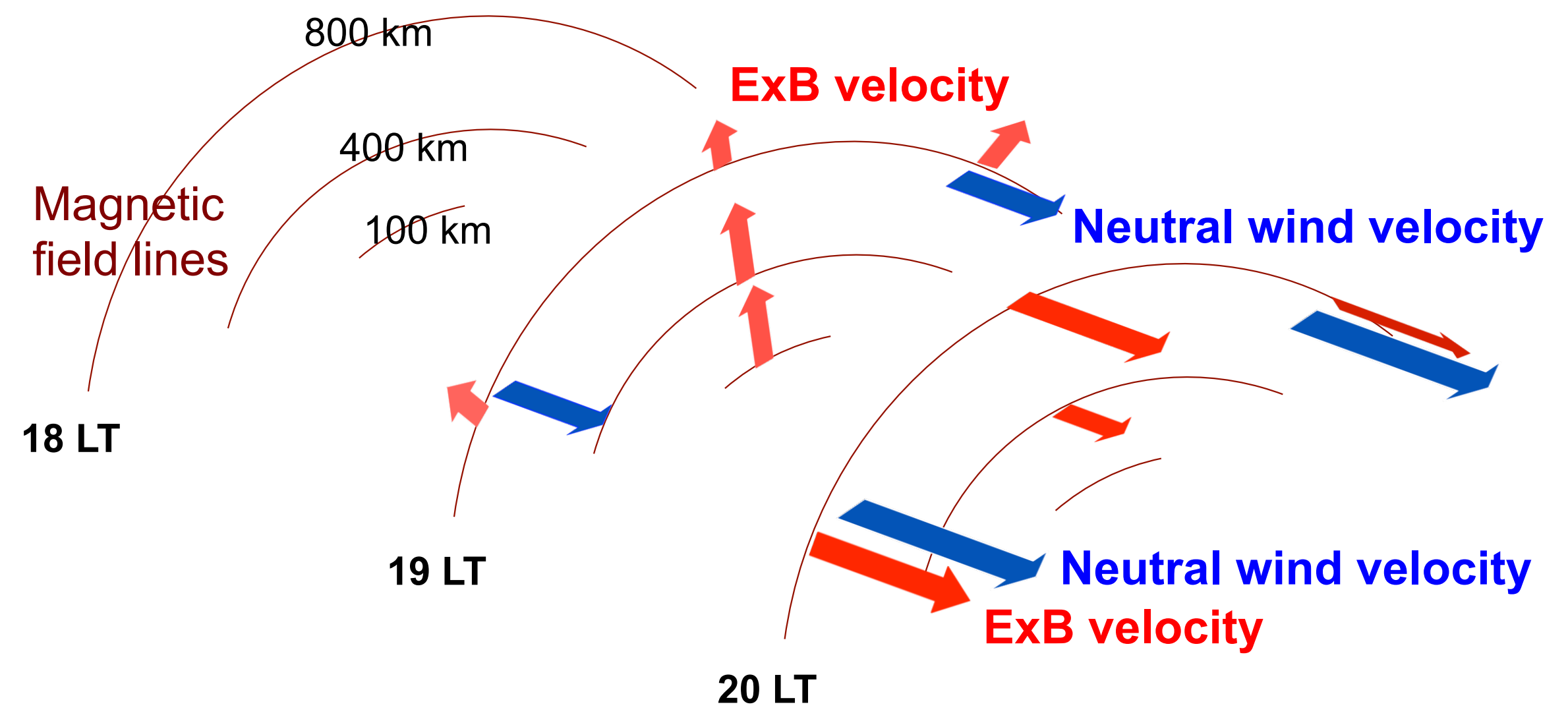

2. Schematic of low-latitude evening neutral wind and ExB convection velocities.

- ExB convection perpendicular to **B** is practically constant along magnetic field lines and flows along electric-potential contours (shown in Figures 6 and 8).
- Convection is driven by wind through ion-neutral collisions.
- Eastward neutral wind increases with height and toward the east, tending to drag plasma along; strongest ion-neutral coupling is at EIA latitudes.
- Eastward ExB velocity increases toward the east for apex heights > 400 km.
- Continuity of ExB convection requires vertical inflow around 18.5-19 LT, producing pre-reversal enhancement (PRE) of vertical drift around 400 km.
- Upward ExB convection extends through E region, where **JxB** force of night-side equatorial electrojet exerts drag on convection.

$$\underset{\text{Neutral Tendency}}{\frac{\partial u}{\partial t}} + \underbrace{\frac{u}{R\cos\lambda}\frac{\partial u}{\partial\phi} + \frac{v}{R}\frac{\partial u}{\partial\lambda} + w\frac{\partial u}{\partial z}}_{\text{momentum advection (small; not shown)}} \underset{\text{Coriolis acceleration}}{- fv} = \underset{\text{Pressure Gradient}}{\frac{-1}{\rho R\cos\lambda}\frac{\partial p}{\partial\phi}} \underset{\text{Ion Drag}}{- \nu_{ni}(u-u_i)} + \underset{\text{Viscosity}}{\frac{1}{\rho}\frac{\partial}{\partial z}\left(\mu\frac{\partial u}{\partial z}\right)}$$

u eastward wind	t time
u_i ion velocity	λ latitude
v northward wind	ϕ longitude
f Coriolis param.	z altitude
ν_{in} drag coef.	R Earth radius + z
μ viscous coef.	ρ mass density
p pressure	

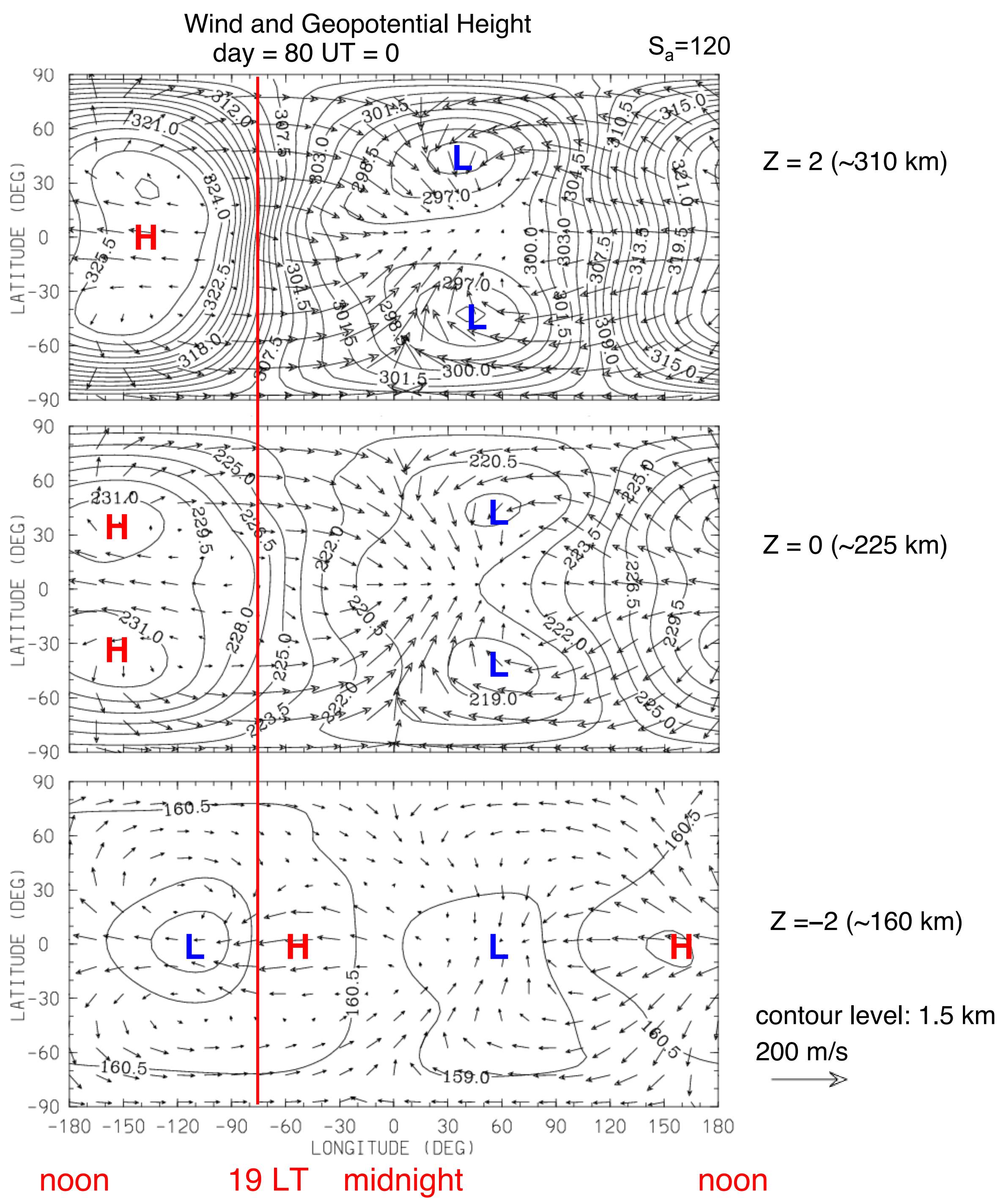

3. Contours show geopotential heights (km) and arrows show horizontal wind velocities (scale at lower right) for TIEGCM pressure levels Z = −2, 0, 2 for the base case simulation at 0 UT. **H** and **L** denote pressure highs and lows. The vertical red line at 75°W longitude is at 19 LT, which is the longitude shown in the figure above and in the vertical profile plots of acceleration, velocity, and drag coefficient.

- At Z=2 and Z=0 the variations have a dominant longitudinal wavenumber 1 (migrating diurnal tide), and the pressure-gradient force is eastward at 19 LT, increasing with height.
- At Z=-2 the variations are have a dominant longitudinal wavenumber 2 (migrating semidiurnal tide), and the pressure-gradient force is westward at 19 LT.
- At 19 LT there is a strong vertical shear of the zonal wind at low latitudes, with a reversal around Z=0.

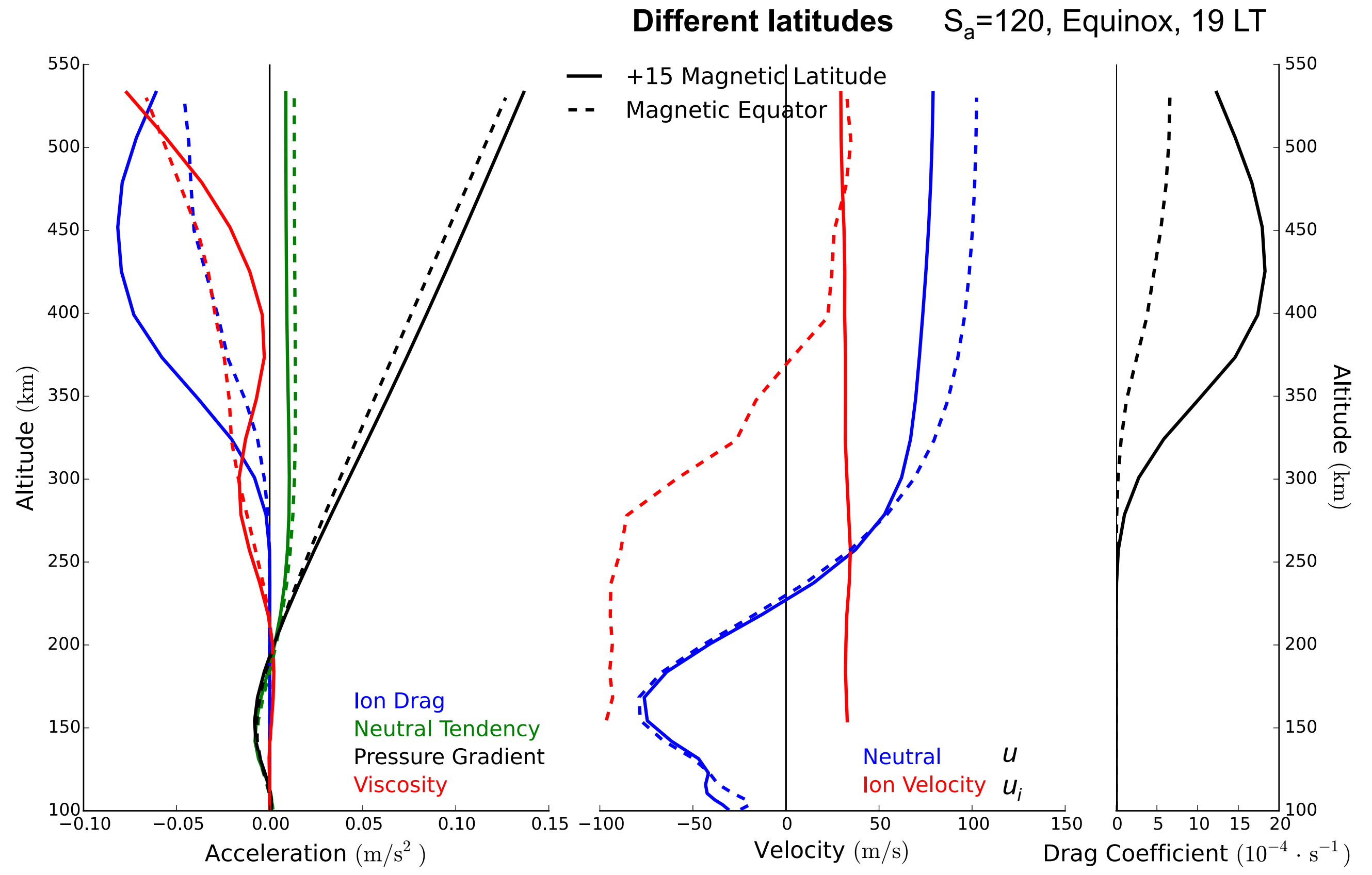

4. (left) Eastward acceleration terms, (middle) eastward neutral and E×B (“Ion”) velocities, and (right) ion-drag coefficient for equinox, medium solar activity, at 75°W geographic longitude, 0 UT (19 LT), for two latitudes. Solid and dashed lines are for +2.5° and −12.5° geographic latitude (+15° and 0° magnetic latitude), respectively.

- Neutral wind tendency is relatively small.
- Horizontal pressure gradient acceleration is similar at both latitudes, increasing with height.
- Pressure gradient is approximately balanced by sum of ion drag and viscosity, differently at the two latitudes.
- Drag coefficient (right panel) and ion drag acceleration are much larger at 15° than at 0° magnetic latitude.
- Strong neutral wind shear exists between 180-250 km.
- Ion velocity varies strongly with height at magnetic equator, but only weakly at 15° magnetic latitude.

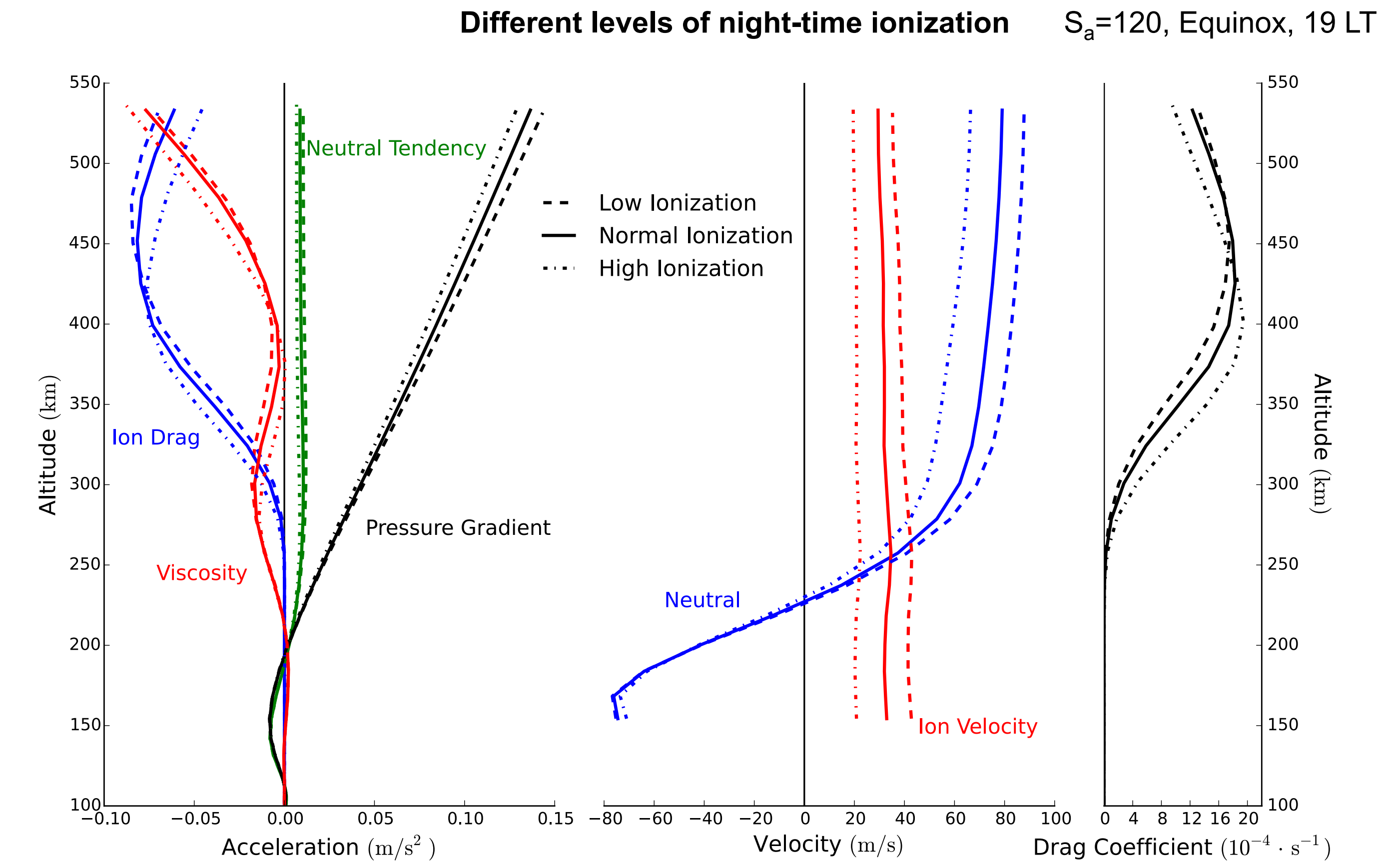

5. (left) Eastward acceleration terms, (middle) eastward neutral and E×B (“Ion”) velocities, and (right) ion-drag coefficients at 2.5° geographic latitude (15° magnetic latitude), 75° W geographic longitude, 0 UT (19 LT), for different levels of nighttime ionization. Solid lines are our base case and the dashed and dash-dotted lines are for lower (x0.1) and higher (x10) nighttime ionization, respectively.

- Ion velocity and F-region neutral velocity vary inversely with E-region conductivity.
- Difference between F-region ion and neutral velocities is similar for all three cases, such that ion drag is also similar. This supports Rishbeth’s [1971] hypothesis that ion drag due to F-region meridional electric current tends to balance pressure gradient.

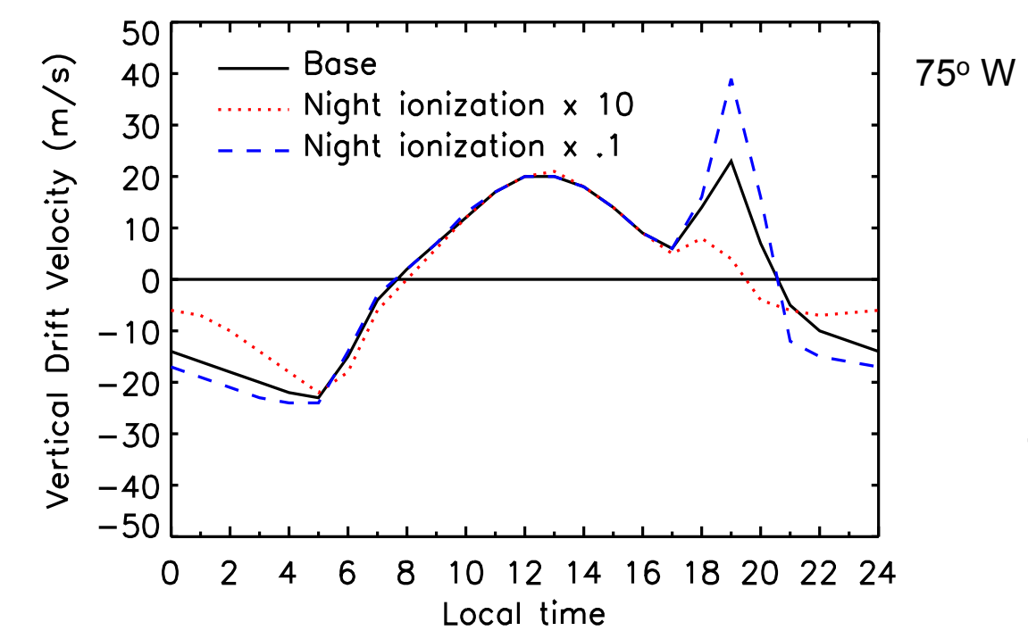

7. Vertical drift velocity at 75°W geographic longitude, 300 km over the magnetic equator, for three levels of nighttime ionization.

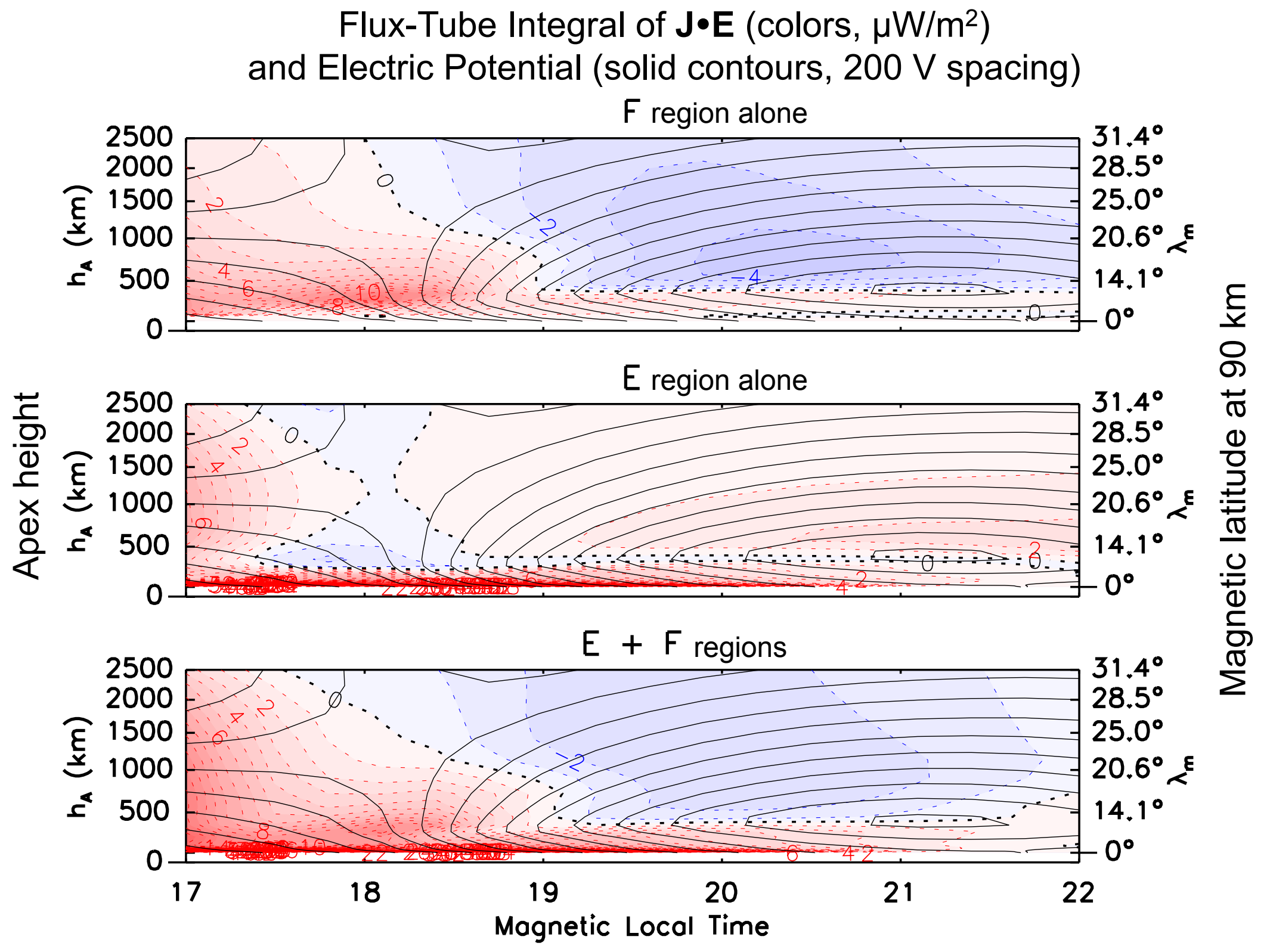

6. Electromagnetic energy dissipation rate integrated along magnetic flux tubes (colors and dashed lines), with overlain electric-potential contours (solid black lines)

- Total area-integrated dissipation between two complete equipotential contours must be zero.
- Energy source (negative dissipation) for the evening plasma convection comes from F region (above 150 km altitude), mainly for h_A > 350 km after 19 MLT.
- Dissipation is strong in electrojet region, h_A<130km, and in PRE region, h_A~300km.

Equinox, S$_a$=120

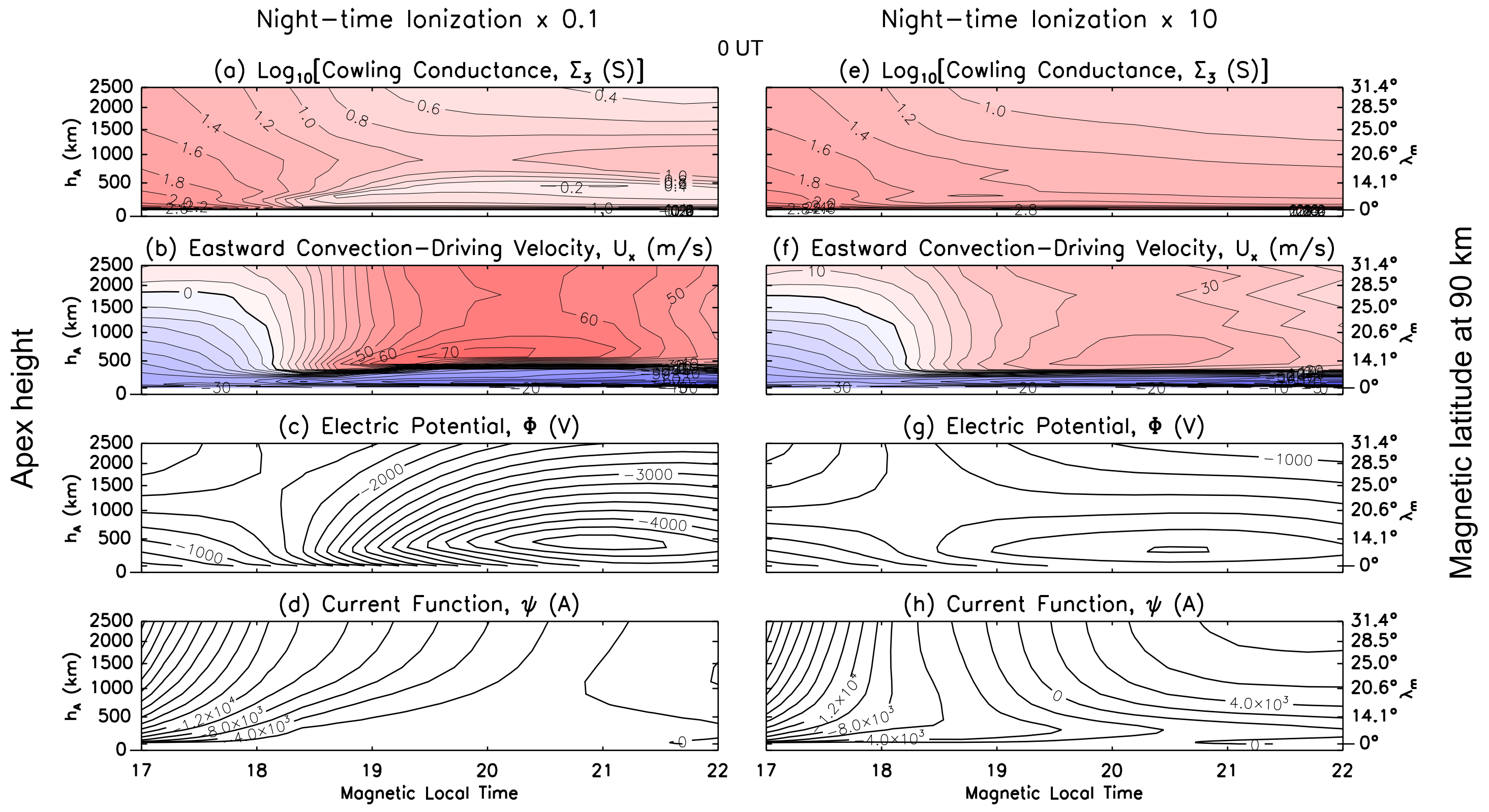

8. Electrodynamic parameters along field lines, for base-case nighttime ionization rate multiplied by 0.1 (left) or 10 (right).

- Reduced E-region ionization (left) allows stronger night-time plasma convection along contours of Electric Potential, increasing pre-reversal enhancement of vertical drift and height of night-time F-region ionosphere (seen in the Cowling conductance). Increased E-region ionization (right) has the opposite effect.
- Eastward Convection-Driving Velocity U_x (=Pedersen-weighted field-line-averaged neutral zonal wind) changes with zonal ion velocity, such that field-line-integrated meridional current tends to be maintained on field lines with apex heights above 800 km (seen in horizontal spacing of Current Function contours).

Evonosky, W., A.D. Richmond, T.-W. Fang, and A. Maute (2016), Ion-neutral coupling effects on low-latitude thermospheric evening winds, J. Geophys. Res. Space Physics, doi:10.1002/2015JA022382.

Richmond, A.D., T.-W. Fang, and A. Maute (2015), Electrodynamics of the equatorial evening ionosphere: 1. Importance of winds in different regions. J. Geophys. Res. Space Physics, 120, 2118-2132. doi:10.1002/2014JA020934.

Richmond, A.D., and T.-W. Fang (2015), Electrodynamics of the equatorial evening ionosphere: 2. Conductivity influences on convection, current, and electrodynamic energy flow. J. Geophys. Res. Space Physics, 120, 2133-2147. doi:10.1002/2014JA020935.

The National Center for Atmospheric Research is sponsored by the National Science Foundation.